J. Appl. Cryst. (1998). **31**, 198–203

A (2 + 3)-Type Surface Diffractometer: Mergence of the *z*-Axis and (2 + 2)-Type Geometries

ELIAS VLIEG†

FOM-Institute for Atomic and Molecular Physics, Kruislaan 407, 1098 SJ Amsterdam, The Netherlands.
E-mail: vlieg@sci.kun.nl

(*Received 14 April 1997; accepted 7 July 1997*)

Abstract

It is shown that the addition of an azimuthal detector rotation to a (2 + 2)-type diffractometer makes it fully equivalent to a *z*-axis type. Using this equivalence, the geometric correction factors for this (2 + 3)-type diffractometer, which are needed to obtain structure factors from measured integrated intensities, are derived. The (2 + 3)-circle diffractometer combines the ideal resolution behaviour of a *z*-axis diffractometer with the mechanical simplicity and range of a (2 + 2)-circle diffractometer. For sample alignment, two additional degrees of freedom are needed, leading to a total of seven circles.

1. Introduction

With the availability of synchrotron radiation sources, surface X-ray diffraction has become an important technique for the structural and morphological characterization of surfaces and interfaces (Feidenhans'l, 1989; Robinson, 1991; Vlieg & Robinson, 1992). The necessary equipment consists of a (vacuum) sample chamber connected to a diffractometer. Because of the horizontal polarization of the synchrotron beam, one usually chooses a horizontal-axis diffractometer in which the surface is mounted vertically, as this avoids near-zero polarization factors for scattering angles near 90°. The horizontal divergence of the synchrotron beam is often larger than the vertical one (particularly for wiggler and bending magnet sources). The horizontal-axis geometry therefore also aligns the diffuse surface diffraction rods with the direction of largest divergence, thus giving an optimum in-plane resolution.

In surface or interface diffraction one requires accurate control over the in- and outgoing angles, while the resolution function is also an important parameter. In addition, a large range of perpendicular momentum transfer is needed. Many diffractometer types are in use that fulfil these requirements in different ways: *z*-axis (Bloch, 1985), five-circle (Vlieg *et al.*, 1987), six-circle (Lohmeier & Vlieg, 1993) and (2 + 2) types (Evans-Lutterodt & Tang, 1995; Renaud *et al.*, 1995). In this paper we show that two common geometries, *z*-axis and (2 + 2)-circle, can be made fully equivalent by the addition of an azimuthal degree of freedom to the detector. This leads to a versatile and convenient geometry for which we also derive the necessary correction factors to obtain structure factors from measured integrated intensities.

2. Conversion of angles

The *z*-axis and (2 + 2)-circle geometries are shown schematically in Figs. 1 and 2. Both have four degrees of freedom: δ and γ for the detector motion and ω for the sample, while α is for sample only [(2 + 2) diffractometer] or for both sample and detector (*z*-axis type). In general, one requires for both types of diffractometer two additional degrees of freedom in order to align the surface normal along the *z* axis. Assuming this alignment has been performed, for both diffractometers the angle of incidence is set by α, while ω sets the sample azimuth. The difference between the two types lies in the reversed order of the δ and γ circles, and the fact that the detector motion is decoupled from α in the (2 + 2) geometry.

The angle settings are found by requiring that the diffraction condition is fulfilled, *i.e.* that the momentum transfer $\mathbf{Q}$ equals a reciprocal-lattice point $\mathbf{H}$:

$$\mathbf{Q} = \mathbf{K}_f - \mathbf{K}_i = \mathbf{H}, \tag{1}$$

with $\mathbf{K}_f$ ($\mathbf{K}_i$) the wavevector of the outgoing (incoming) beam. The reciprocal-lattice point is given by $\mathbf{H} = h\mathbf{b}_1 + k\mathbf{b}_2 + l\mathbf{b}_3$, where ($hkl$) are the Miller indices and $\mathbf{b}_i$ the reciprocal-lattice vectors. As a convention, the Miller index l will be used to denote the direction of perpendicular momentum transfer $\mathbf{Q}_\perp$, while h and k define the in-plane momentum transfer $\mathbf{Q}_\parallel$. The solution of (1) with the appropriate boundary condition of fixed incoming or outgoing angle has been given by Bloch (1985) and Lohmeier & Vlieg (1993), for the *z*-axis diffractometer, and by Evans-Lutterodt & Tang (1995) for the (2 + 2) geometry.

Here we only need to consider the detector position, since the sample orientation angles α and ω are iden-

† Present address: Research Institute for Materials, Department of Solid State Chemistry, University of Nijmegen, Toernooiveld 1, 6525 ED Nijmegen, The Netherlands.

tical for both cases. In the laboratory frame, the direction of the outgoing beam is given by

$$\frac{\mathbf{K}_f}{K} = \mathbf{A}\Delta_z\Gamma_z\begin{pmatrix}0\\1\\0\end{pmatrix} \tag{2}$$

for the z-axis machine, and by

$$\frac{\mathbf{K}_f}{K} = \Gamma_{2+2}\Delta_{2+2}\begin{pmatrix}0\\1\\0\end{pmatrix} \tag{3}$$

for the $(2+2)$-type diffractometer. The rotation matrices in these equations are (see Fig. 1)

$$\mathbf{A} = \begin{pmatrix}1 & 0 & 0\\ 0 & \cos\alpha & -\sin\alpha\\ 0 & \sin\alpha & \cos\alpha\end{pmatrix}, \tag{4}$$

$$\Delta_i = \begin{pmatrix}\cos\delta_i & \sin\delta_i & 0\\ -\sin\delta_i & \cos\delta_i & 0\\ 0 & 0 & 1\end{pmatrix} \tag{5}$$

and

$$\Gamma_i = \begin{pmatrix}1 & 0 & 0\\ 0 & \cos\gamma_i & -\sin\gamma_i\\ 0 & \sin\gamma_i & \cos\gamma_i\end{pmatrix}, \tag{6}$$

where the label i stands for z or $(2+2)$. The condition that the detector position is equivalent for both geometries means that the right-hand sides of (2) and (3) should be equal

$$\mathbf{A}\Delta_z\Gamma_z\begin{pmatrix}0\\1\\0\end{pmatrix} = \Gamma_{2+2}\Delta_{2+2}\begin{pmatrix}0\\1\\0\end{pmatrix}. \tag{7}$$

Expanding this, one finds

$$\begin{pmatrix}\sin\delta_z\cos\gamma_z\\ \cos\delta_z\cos\gamma_z\\ \sin\gamma_z\end{pmatrix} = \begin{bmatrix}\sin\delta_{2+2}\\ \cos(\gamma_{2+2}-\alpha)\cos\delta_{2+2}\\ \sin(\gamma_{2+2}-\alpha)\cos\delta_{2+2}\end{bmatrix}. \tag{8}$$

From this one easily derives the following relations which convert z-axis angles into $(2+2)$ ones and *vice versa*:

$$\sin\delta_{2+2} = \sin\delta_z\cos\gamma_z, \tag{9}$$

$$\tan(\gamma_{2+2}-\alpha) = \tan\gamma_z/\cos\delta_z, \tag{10}$$

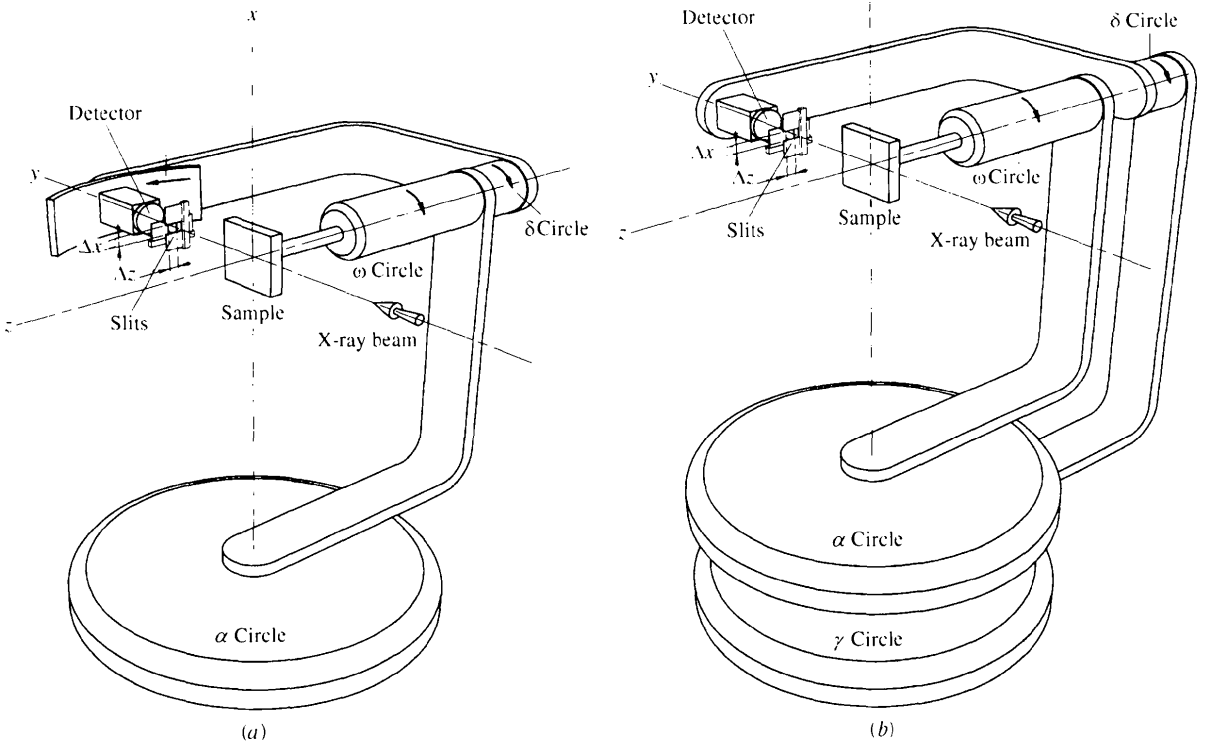

Fig. 1. Schematic of (*a*) a z-axis diffractometer and (*b*) a $(2+2)$-circle diffractometer. All circles are shown at zero position. The slits are shown in front of the detectors.

$$\tan\delta_z = \tan\delta_{2+2}/\cos(\gamma_{2+2} - \alpha) \quad (11)$$

and

$$\sin\gamma_z = \cos\delta_{2+2}\sin(\gamma_{2+2} - \alpha). \quad (12)$$

The angle of incidence α will be known in all cases. Since γ_z equals the outgoing angle in the z-axis mode, (12) immediately gives an expression for the outgoing angle β_{out} for the (2 + 2)-circle diffractometer,

$$\sin\beta_{out} = \cos\delta_{2+2}\sin(\gamma_{2+2} - \alpha). \quad (13)$$

3. Detector rotation

The direction of the outgoing wavevector is determined by two angles; thus it is possible to convert the z-axis and the (2 + 2)-type angles into each other using the two available degrees of freedom. However, the two diffractometers are still not completely equivalent because a detector will always be equipped with slits (or an analyzer crystal plus slit) that define the angular acceptance. As Fig. 2 shows, even when using the equivalent detector angles, the azimuth of the detector slits is not the same for the two types of diffractometer. It will now be shown how this last difference can be removed.

When all angles are set to zero, the slit settings are identical (see Fig. 1). The slit openings will be termed Δx and Δz for the x and z directions, respectively. With all angles set to zero, Δz fully determines the amount of accepted perpendicular momentum transfer $\mathbf{Q}_\perp$; Δx has no influence on this. For the z-axis diffractometer this remains true for nonzero angles because the δ and γ circles are located such that $\Delta x \perp \mathbf{Q}_\perp$. For the (2 + 2) type, however, nonzero δ and γ values do lead to an influence of Δx, and corrections for the amount of intercepted rod become necessary (Evans-Lutterodt & Tang, 1995; Renaud *et al.*, 1995).

In order to make the z-axis and (2 + 2)-type diffractometers fully equivalent, one therefore has to add an azimuthal rotation to the detector (see Fig. 3). One then obtains a (2 + 3)-type diffractometer. The angle setting v for this azimuth is found by requiring that $\Delta x \perp \mathbf{Q}_\perp$. In the surface frame, this condition becomes

$$\mathbf{A}^{-1}\Gamma_{2+2}\Delta_{2+2}\mathbf{N}\begin{pmatrix}1\\0\\0\end{pmatrix}\begin{pmatrix}0\\0\\1\end{pmatrix} = 0, \quad (14)$$

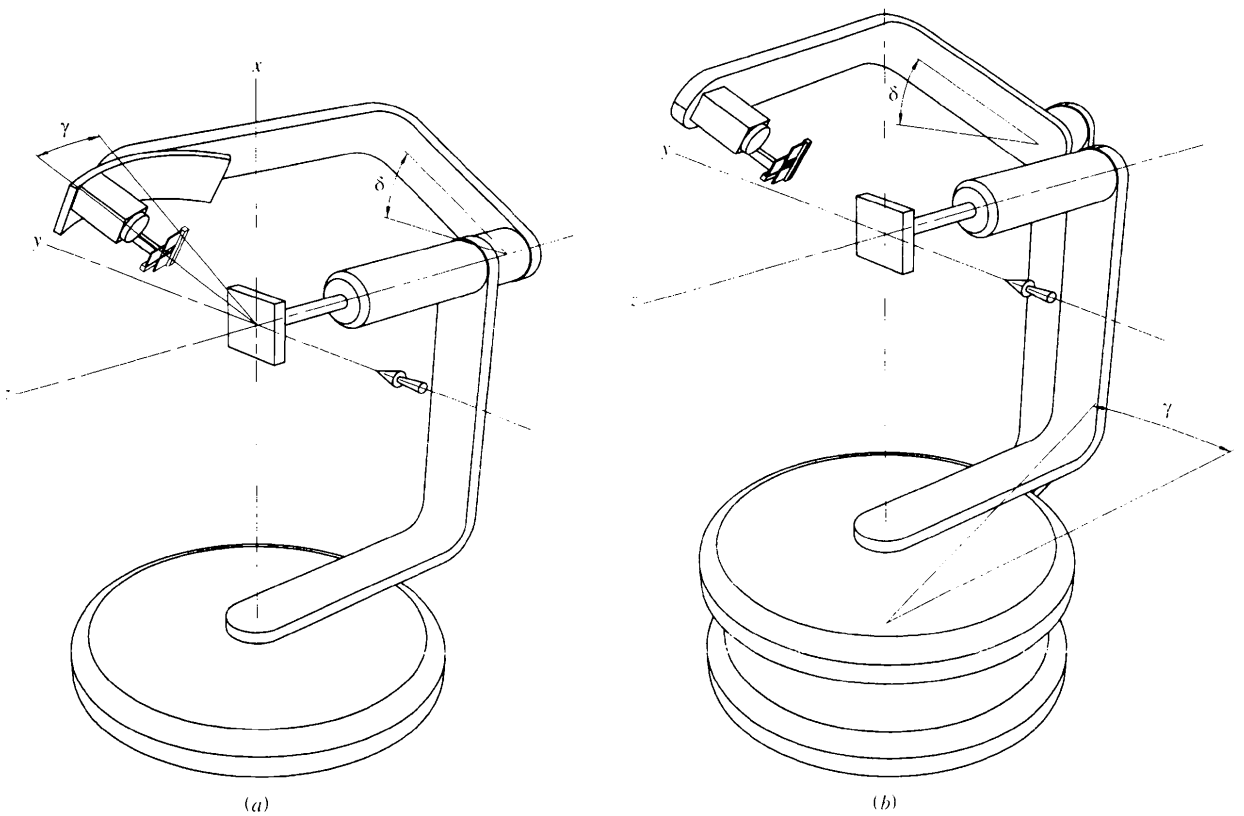

Fig. 2. Schematic of (*a*) a z-axis and (*b*) a (2 + 2)-circle diffractometer for nonzero detector angles. The angles are taken such that the settings are equivalent. The figure shows that even in this case the azimuthal orientation of the slits is different.

with

$$\mathbf{N} = \begin{pmatrix} \cos\nu & 0 & \sin\nu \\ 0 & 1 & 0 \\ -\sin\nu & 0 & \cos\nu \end{pmatrix}. \quad (15)$$

This leads to

$$\tan\nu = -\tan(\gamma_{2+2} - \alpha)\sin\delta_{2+2}, \quad (16)$$

from which the angle ν is readily calculated. This, together with (9) to (12), gives a complete mapping of the (2 + 3)-type diffractometer on the z-axis machine.

4. Integrated intensities

In order to derive structure factors from measured integrated intensities, various correction factors have to be applied that depend on the type of diffractometer used. Vlieg (1997) has derived these for a six-circle diffractometer for which the z axis is a special (and simple) case. By using the conversion relations derived above [(9)–(12)], we can now use these z-axis results to derive easily the correction factors for the (2 + 3)-type diffractometer.

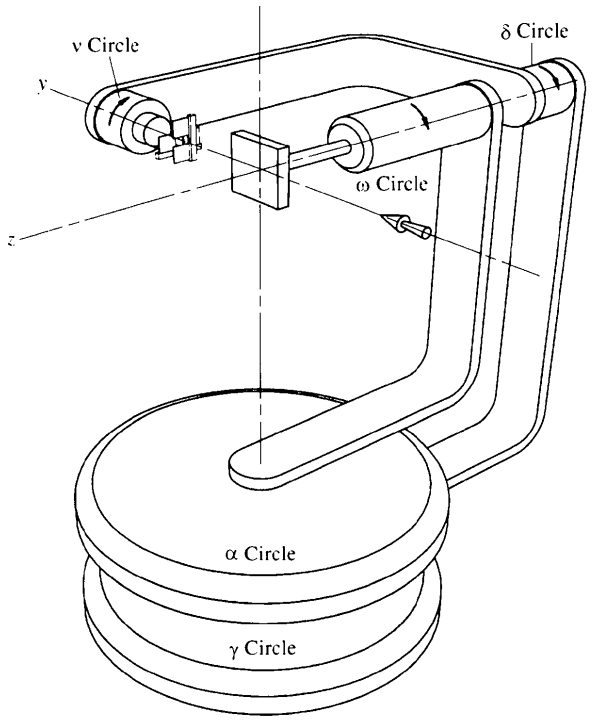

Fig. 3. Schematic of a (2 + 3)-circle diffractometer. This has the same geometry as the (2 + 2)-type, but with the addition of a ν circle for the azimuth of the detectors and slits.

Following the same notation as in Vlieg (1997), we write for the integrated intensity in a rocking or ω scan

$$I_{\mathrm{int},\omega} = \frac{\Phi_0 r_e^2 A_0 \Delta\rho}{\omega_0 A_u^2} |F_{hkl}|^2 L_\omega P C_{\mathrm{rod}} C_{\mathrm{area}} C_{\mathrm{det}} C_{\mathrm{beam}}, \quad (17)$$

with Φ_0 the incident flux, r_e the classical electron radius, A_0 the angle-independent part of the active surface area, $\Delta\rho$ the angular acceptance along the slit z direction, ω_0 the rotation speed, A_u the unit-cell area and F_{hkl} the structure factor. The other terms are the correction factors we are concerned with here. L_ω is the Lorentz factor for an ω scan, P the polarization factor and C_{rod} the correction factor for the rod interception. C_{area} determines the variation in the active sample area, C_{det} corrects for a finite in-plane detector acceptance and C_{beam} is the correction factor for a finite beam size.

The factors C_{det} and C_{area} are the same as those given in Vlieg (1997) and thus will not be discussed here. Converting the z-axis results to the (2 + 3) situation, we find for the Lorentz factor for ω scans

$$L_\omega = 1/\sin\delta_{2+2}\cos\alpha. \quad (18)$$

Since the δ values for the (2 + 2) and (2 + 3) geometries are the same, we will simply continue to write δ_{2+2}. The polarization factor is

$$P = p_h P_{\mathrm{hor}} + (1 - p_h) P_{\mathrm{ver}}, \quad (19)$$

with p_h the horizontal polarization fraction of the beam, and where

$$P_{\mathrm{hor}} = 1 - \sin^2\gamma_{2+2}\cos^2\delta_{2+2} \quad (20)$$

and

$$P_{\mathrm{ver}} = 1 - \sin^2\delta_{2+2} \quad (21)$$

are the polarization factors for the horizontal and vertical beam polarization directions, respectively. The area correction is found to be

$$C_{\mathrm{area}} = \cos\beta_{\mathrm{out}}/\sin\delta_{2+2}, \quad (22)$$

while the rod interception correction is given by

$$C_{\mathrm{rod},2+3} = \cos\beta_{\mathrm{out}}. \quad (23)$$

These expressions thus allow structure factors to be derived from ω scans. Integrated intensity measurements without moving the sample or detector were also discussed in Vlieg (1997) and the corresponding correction factors can be found in a manner analogous to the one used above.

For a (2 + 2)-type diffractometer (*i.e.* no ν rotation) the correction factors are the same, except for C_{rod}. As was discussed by Evans-Lutterodt & Tang (1995), for a (2 + 2)-type diffractometer the amount of intercepted rod may not only be limited by Δz, but also by Δx when

the slits are rotated. Under the assumption that the amount of intercepted rod is limited by Δz, we can derive $C_{\rm rod}$ in the same manner as discussed in Vlieg (1997), for the six-circle diffractometer: one has to calculate the cross section of the plane that the diffraction rod traces during an ω scan, with the lines that define the detector aperture at $\pm \frac{1}{2}\Delta z$. After some arithmetic, this leads to

$$C_{\rm rod,2+2} = \cos\alpha[_{2+2}\sin^2(\alpha - \gamma_{2+2})\cos\delta_{2+2} + \cos\alpha\cos(\alpha - \gamma)_{2+2}]^{-1}. \quad (24)$$

5. Discussion and conclusion

A number of the correction factors derived above were also discussed by Evans-Lutterodt & Tang (1995), where explicit formulae were given for the special cases of $\beta_{\rm out} = 0$ or $\alpha = \beta_{\rm out}$. Our results are more general, but are consistent with those of Evans-Lutterodt & Tang (1995), except for the rod interception correction factor $C_{\rm rod,2+2}$. Our equation (24) differs from their result for the case of $\alpha = \beta_{\rm out}$. One reason for this discrepancy could be that Evans-Lutterodt & Tang considered the projected lengths of the slit openings. Since Δx is not perpendicular to $\mathbf{Q}_\perp$, the total intercepted rod length is not simply a projection. The numerical difference between the two results, however, is only a few percent for small values of δ_{2+2}.

Since the difference between a (2 + 2)- and a (2 + 3)-type diffractometer appears only to be a difference in the $C_{\rm rod}$ correction, the question arises whether the extra costs and complication of a ν rotation are really justified. We think they are for the following reasons.

(i) $C_{\rm rod,2+2}$, as given in (24), only deals with the case whereby Δz determines the effective rod interception. In general, one also needs to consider the situation where Δx becomes the limiting slit. This will certainly be the case with δ_{2+2} values close to 90°. In the (2 + 2) geometry, one therefore has the situation that $C_{\rm rod}$ and the resolution vary greatly for measurements at different points in reciprocal space.

(ii) An analyzer crystal may be used to obtain a high $Q_\parallel$ resolution. However, for out-of-plane data using the (2 + 2) geometry, the rotation with respect to the diffraction rods will lead to an immediate loss in this resolution, while at the same time the small angular acceptance will start to limit the amount of intercepted rod.

(iii) When a position-sensitive detector is used [*e.g.* a CCD (charge-coupled device) camera], it is convenient to preserve the $\mathbf{Q}_\parallel$ and $\mathbf{Q}_\perp$ directions in the detector read-out. This is not possible in the (2 + 2) geometry.

Depending on the use of the diffractometer, there are thus many cases in which the ν rotation has advantages.

Next we consider the difference between a z-axis and a (2 + 3) diffractometer. From the point of view of angle settings, the z-axis geometry is the most intuitive and convenient. The (2 + 3) diffractometer appears again to have one extra degree of freedom, while the settings and corrections are equivalent to a genuine z axis. However, in order to implement a z-axis machine, one often relies on a linear translation plus a rotation stage, which also needs mechanical support for sufficient stability. The six-circle diffractometer of Ferrer & Comin (1995) has, for example, a counter detector circle for this purpose, leading to a total of three axes to implement an effective γ circle. Compared to such a case, the (2 + 3) configuration is a simpler alternative, with the added benefits that the detector–sample distance remains constant and that larger γ values can be achieved. Other implementations of a z-axis diffractometer do exist which do not have these limitations, but which are more restrictive in the size of sample chamber allowed (Feidenhans'l, 1997).

Another potential benefit of the (2 + 3) diffractometer with respect to a z-axis machine occurs when the same machine is also used in a horizontal scattering geometry. This would require extra degrees of freedom for the sample, either on the ω circle or on top of the α table, but the detector geometry of the (2 + 3)-circle diffractometer is already ideal, because the sample and detector motions are fully decoupled. This leads to a simpler operation without the need to have multiple axes move in the most common scans, unlike the z-axis geometry. A disadvantage of the (2 + 3) geometry is that the γ circle increases the diffractometer height with respect to a z-axis one, which may lead to space problems.

As mentioned above, one needs two additional degrees of freedom on the sample in order to align the surface normal with the z axis. These can either be two tilt stages, or one tilt stage together with a rotation axis. When using a z-axis geometry the two options are equivalent, but the rotation/tilt combination does allow the diffractometer to be used in a six-circle mode, which enhances the area of reciprocal space that can be accessed (Lohmeier & Vlieg, 1993). A complete horizontal-axis diffractometer would thus in total require seven degrees of freedom, in a (4 + 3) geometry, of which only (2 + 3) are needed after the initial sample alignment.

In conclusion, we have shown that the (2 + 3)-circle diffractometer combines the best properties of the z-axis and (2 + 2) geometries for surface X-ray diffraction. It has a well defined resolution function, a large accessible range in reciprocal space and is mechanically simple. By using the equivalence with the z-axis geometry, we derived the geometric correction factors necessary to extract structure factors from measured integrated intensities. A diffractometer of this type will be installed at the Dutch–Belgian beamline (DUBBLE)

at the European Synchrotron Radiation Facility (ESRF) in Grenoble, France.

I thank I. Cerjak for drawing the figures, and W. H. de Jeu and S. A. de Vries for critical reading of the manuscript. This work is part of the research programme of the Foundation for Fundamental Research on Matter (FOM) and was made possible by financial support from the Netherlands Organization for Scientific Research (NWO).

References

Bloch, J. M. (1985). *J. Appl. Cryst.* **18**, 33–36.
Evans-Lutterodt, K. W. & Tang, M.-T. (1995). *J. Appl. Cryst.* **28**, 318–326.
Feidenhans'l, R. (1989). *Surf. Sci. Rep.* **10**, 105–188.
Feidenhans'l, R. (1997). Personal communication.
Ferrer, S. & Comin, F. (1995). *Rev. Sci. Instrum.* **66**, 1674–1676.
Lohmeier, M. & Vlieg, E. (1993). *J. Appl. Cryst.* **26**, 706–716.
Renaud, G., Villette, B. & Guénard, P. (1995). *Nucl. Instrum. Methods*, **B95**, 422–430.
Robinson, I. K. (1991). *Handbook on Synchrotron Radiation*, Vol. 3, edited by G. S. Brown & D. E. Moncton, pp. 221–266. Amsterdam: North-Holland.
Vlieg, E. (1997). *J. Appl. Cryst.* **30**, 532–543.
Vlieg, E. & Robinson, I. K. (1992). *Synchrotron Radiation Crystallography*, edited by P. Coppens, pp. 255–299. London: Academic Press.
Vlieg, E., van der Veen, J. F., Macdonald, J. E. & Miller, M. (1987). *J. Appl. Cryst.* **20**, 330–337.